Journal of
Nanomedicine & Nanotechnology

Yang et al., J Nanomed Nanotechnol 2016, 7:1
DOI: 10.4172/2157-7439.1000344

Research Article Open Access

An Early Cancer Diagnosis Platform based on Micro-magnetic Sensor Array Demonstrates Ultra-high Sensitivity

Nan Yang, Tao Li, Ping Ping Zhang, Xiaoqiang Chen, Xuefeng Hu* and Wei Zhang*

State of Key Laboratory of Materials-oriented Chemical Engineering and School of Chemical Engineering, Nanjing Tech University, Nanjing, Jiangsu, 210009, PR. China

Abstract

In this paper a highly sensitive detection methodology for obtaining the concentration of protein tumor markers via the selective incorporation of super paramagnetic iron oxide nanoparticles (MNP) onto an antigen is reported. The tumor marker concentration is measured with a nano-oxide layer inserted giant magneto-resistive (GMR) sensor that determines the attenuation of an external magnetic field that is induced by the MNP. The 15 nm MNPs, used herein, exhibit a super paramagnetic behavior with saturation magnetization of 36 emu/g. The output voltage signal of the Specular GMR sensor is 500 μV/Oe. The patterned GMR multiple-bio-sensor array, has demonstrated real-time measurements of carcinoembryonic antigen (CEA) protein concentrations down to femtomole level (10-15 mole) in a variety of clinically relevant media with a linear dynamic range of over five orders of magnitude. The sensitivity of the GMR bio-array platform is 1000 times higher than conventional enzyme-linked immunosorbent assay (ELISA) technique. The arrays of magnetoresistive sensors offer great promise in applications for early cancer diagnosis.

Keywords: Colorectal cancer; Nanoparticles; Protein microarrays; Quantum dots; Superparamagnetic property

Introduction

Colorectal cancer (CRC) is one of the most commonly diagnosed types of cancer worldwide. Carcinoembryonic antigen (CEA) in human serum is reported to be an important biomarker for early CRC diagnosis [1-3]. Because CEA's concentration in human serum is very low (approximately 2.5 ng/mL), a highly sensitive measurement technique for the identification of the presence of CEA is required. Currently Enzyme-linked immunosorbent assay (ELISA) [4,5] is a widely used protein readout method based on a fluorescent or colorimetric transducer response. However, inherent auto fluorescence and optical absorption of either the matrix of biological samples or reagents is a major limiting factor of ELISA technique. Several other technologies, such as, nanowires [6], carbon nanotubes [7], electrochemical biosensors [8], protein microarrays [9], and quantum dots [10], has been also investigated as diagnostic tools for protein detection. The detection physics for these non-optical methods are rooted in charge-based interactions between either the protein or tag and the sensor, which limits the reliability of these sensor types due to solutions of varying pH and ionic strength.

Bio-sensing strategies based on magnetic nanoparticles (MNP) have received considerable attention [11,12]. Magnetic particles possess unique magnetic properties and easily functionalized with stable, nontoxic protective coatings for bioconjugation [13-15]. Magnetic background in biological samples is minimal, since these are composed predominantly of diamagnetic molecules, and even large magnetic fields are compatible with biochemical processes. In particular, the stray magnetic fields from the beads, as well as externally applied field gradients which can be used to generate forces on the beads to remotely manipulate them are not screened in an aqueous biological environment. Tiny size, which exhibits a superparamagnetic property, allows for the formation of stable dispersion in reaction solution, making them well suitable for target separation [14,16,17], targeted delivery of therapeutic agents [18], and biosensor based diagnostics [19].

Among these platforms or concepts using magnetic nano- particle labels and magnetometers, the first demonstration of detecting biological molecules by employing magnetic labels was achieved with superconducting quantum interference device (SQUID) [20]. In 1998, Baselt et al. introduced the bead array counter (BARC) for the detection of a single molecule combined with a magnetic particle [21]. This platform was then developed into a system for biological warfare agents detection [22]. In addition, the efforts paid on substituting giant magnetoresistive (GMR) sensors for traditional magnetic sensors in immunoassay or lab-on-a-chip-based rapid point-of- care testing (POCT) has been significantly increasing [23-25]. Most recent studies [26-35] have demonstrated the usage of GMR biosensors that detect either as few as 600 streptavidin coated magnetic particle (<10-21 mol, zeptomol) or CEA with at lower limit of detection around 50 fM (10-15). For CEA sensing, it is ideal to have the particle labels either 20 nm or smaller in diameter [36]. However, the magnitude of the detectable magnetic field decrease with particle size, thus, a more sensitive sensors and measurement systems is required [37].

In this paper, a low-amount biomarker detectable platform based on a 15 nm diameter MNPs and high sensitive specular giant magnetoresistance (GMR) sensors was investigated. The GMR ratio can be enhanced by nano-oxide layer (NOL) insertion inside the pinned layer. The magnetic particle agglomeration can be avoided due to the superparamagnetism.. The ultra-small size of MNPs can be more comparable to that of the conjugating biomolecules so that they would not block biomolecular interactions. We also demonstrate the feasibility of this detecting system for real biological applications, with the example of the logarithmic detection of CEA, a breast cancer biomarker, through a sandwich-based principle.

***Corresponding authors:** Wei Zhang, State of Key Laboratory of Materials-oriented Chemical Engineering and School of Chemical Engineering, Nanjing Tech University, Nanjing, Jiangsu, 210009, PR. China, Tel: 86 25-83587060; E-mail: zhangw@njtech.edu.cn

Xuefeng Hu, State of Key Laboratory of Materials-oriented Chemical Engineering and School of Chemical Engineering, Nanjing Tech University, Nanjing, Jiangsu, 210009, PR. China, E-mail: xuefeng.hu@njtech.edu.cn

Received November 25, 2015; **Accepted** December 29, 2015; **Published** January 10, 2016

Citation: Yang N, Li T, Zhang PP, Chen X, Hu X, et al. (2016) An Early Cancer Diagnosis Platform based on Micro-magnetic Sensor Array Demonstrates Ultra-high Sensitivity. J Nanomed Nanotechnol 7: 344. doi:10.4172/2157-7439.1000344

Experiment

A specular GMR stack with Ta (1.5 nm)/NiFeCr (3 nm)/PtMn (12 nm)/CoFe (1.8 nm)/Ru (0.85 nm)/CoFe (1 nm)/Nano oxides layers and (NOL, 1.3 nm)/CoFe (2 nm)/Cu (2.1 nm)/CoFe (0.8 nm)/NiFe (1.5 nm)/Cu0.8 nm/Ta (1.2 nm) layers was deposited with a sputtering system (Anelava, JPN). In order to obtain best sensitivity of the sensor, the magnetization of free layer and the pinned layers of the sensor are set perpendicular relative to each other by two annealing steps under magnetic fields with 6 tesla and 500 Oe respectively. GMR sensors with a nominal size of 200 × 150 μm were then created via the optical photolithography technique.

As shown in Figure 1, similar to ELISA, the magnetic arrays require bio-function steps and links prior to real-time measurement. To form the base layer of the bio-functionalization, a 2% solution of polyethyleneimine (PEI) (Shanghai Qunfang Bio) in deionized water was applied to the chip surface. CEA analyte (Shanghai, NC-Bio) was diluted to the desired concentrations in the phosphate buffer saline (PBS). Twenty μL of this solution were selectively pipetted into sensors which were printed by captured antibodies onto sensors blocked by bovine serum albumin (BSA). Biotinylated antibodies to CEA (Ocean Nanotech) were diluted to a concentration of 2 μg/ml in PBS. 20 μL of this linker antibody solution were pipetted onto the surface of each sensor. Finally, 40 μL of streptavidin labeled MNPs (Ocean Nanotech) was added and incubated without stirring for 30 min at room temperature.

The size and morphology of the MNPs were characterized by Transmission Electron Microscopy (TEM). Electron Energy Loss Spectra (EELS) was used to characterize the composition of the streptavidin labeled MNP. The magnetic property measurement of the MNPs was carried out at room temperature by using a Superconducting Quantum Interference Device (SQUID). Analyte quantification was performed on a probe station (KLA-350 A), which used a source meter in a two-point configuration. Local external magnetic fields up to 3000 Oe in either the transverse (hard axis) or longitudinal (easy axis) direction relative to the sensor was generated by a quadarupole magnet [38].

Result

A typical TEM image of the MNPs is presented in Figure 2a. The MNPs exhibit a spherical shape with an average size of around 15 nm. As shown in Figure 2b, the MNPs, characterized by SQUID, display a saturation magnetization of 36 emu/g under a field of more than 40 KOe and 1.01 emu/g at a field of 100 Oe. It is estimated that 1 gram of these 15 nm MNPs will correspond to 2.63 x 1017 particles. The net magnetic moment of single MNP is 6.66 x 10-17 emu at a field of 40 kOe and 3.8 x 10-18 emu at a field of 100 Oe [39]. TEM images of streptavidin-modified nanoparticles, as shown in Figure 2c, demonstrated uniform streptavidin modification with no significant particle aggregation. The iron compositions of streptavidin-modified MNP, as characterized by EELS, as shown in Figure 2d, exhibited a streptavidin uniformly distributed across the MNP particle with no perceivable grain boundary. The aforementioned findings suggest not much significant nonspecific binding of streptavidin to the magnetic nanoparticles.

Each layer of secular GMR stack, as shown at Figure 3, has an nm-level thickness with sharp interface between layers. Magnetoresistance ratio (MR) ratio for the full-film specular GMR sensor, measured by the field strength along the hard axis (transverse), is about 16% with a maximum sensitivity of 1.6% Oe-1 at 10 Oe field. Very slight hysteresis is shown in the loop for full film specular GMR [37,38,40,41]. The optical image of patterned specular GMR bioarrary is shown at Figure 4a. Each sensor was patterned into a square shape with 200 μm × 200 μm dimensions. After electrode deposition (250 μm × 25 μm), each sensor occupies an active area of 200 μm by 150 μm while the edge to edge distance of two sensors' separation is 100 μm. The resistance of each sensor is about 1.1 K Ω under a zero field.

To achieve statistically reliable results, for the CEA detection experiments, five sensors were selected. The concentration of CEA was about 500 femtomole (1 ng/mL, 1 μL droplet). The aforementioned second group of 5 sensors acted as negative controls. The MR loops of specular GMR sensors with CEA analyte and sensor blocked by BSA were measured before and after the spiking of the streptavidin labeled MNPs. As shown on Figure 4b, all curves exhibited giant magnetoresistance (GMR). The dR/R was 10.03% and 8.99% for patterned sensors before and after the MNPs was spiked, respectively. In contrast, a 10.01% dR/R was measured for sensors with BSA blocking under the hard-axis bias condition. Shape anisotropy due to the patterned rectangle GMR sensor caused hysteresis to appear in the loop in the transverse curve. The dR/R ratio changes before and after magnetic particle incorporation is used to identify low amounts of biomolecules. The sensitivity of the sensor before MNPs spiking is around 0.5%/Oe (and 500 μV/Oe). Each dipole moment generated from magnetic particle creates a small added field component Hdipole at the sensor. The sensor will experience an effective field strength which is slightly smaller than the external applied field (Heffect = Happlied − Hdipole). This effect generates a detectable signal on the GMR sensor arrays, normally a decrease in dR/R. The signal levels of 500 femtomole CEA is 5 × 104 μV, which is significantly larger and distinct from the nonspecific signal of 15 μV on the sensor blocked

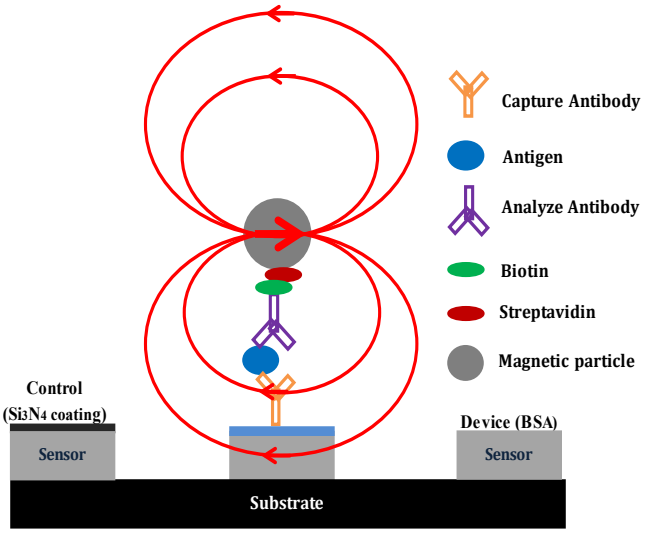

Figures 1: A cartoon of the GMR bioassay: (1) Capture antibodies (yellow) are immobilized onto the surface of the sensor; (2) The chosen antigens (CEA in the present case, blue) are complementary to the capture antibodies (yellow) and the non complementary antigens are subsequently washed away; (3) The biotinylated detection antibody (purple) complementary to the antigen of interest binds in a sandwich structure and the non complementary antibodies are washed away. (4) A streptavidin (deep red) labeled MNPs (black) are added to the solution, and it binds the biotinylated detection antibody. Unbounded streptavidin labeled SPION is removed by an applied magnetic field. (5) Finally, the magnetic fields from the magnetic nanoparticles binding to detection antibody can be detected by the underlying GMR sensor in real-time with the presence of a small external modulation magnetic field.

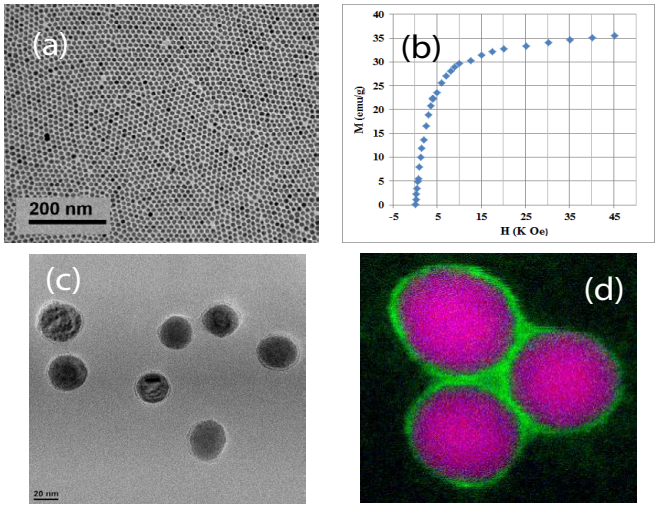

Figure 2: (a) TEM bright-field image for the spherical iron–oxide MNPs with an average diameter of 20 nm; (b) SQUID measurement of the MNP. The saturation magnetization is 36 emu/g; (c) TEM images of MNP particles modified by streptavidin, indicating no significant particle aggregation; (d) EELS composition analysis of streptavidin labeled MNP, suggesting uniform Fe distribution across MNP particles and carbon across the streptavidin coating.

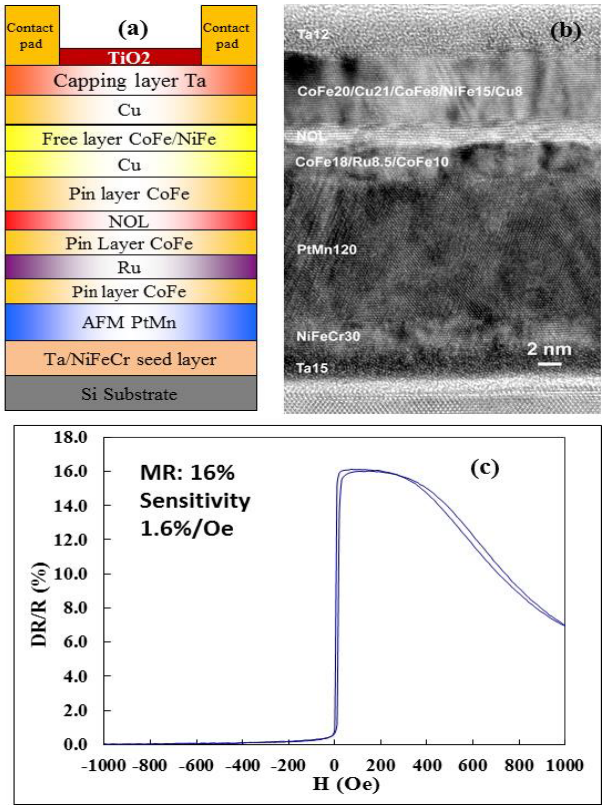

Figure 3: The scheme and TEM image of a full film specular GMR stack and transvers curve. (a) The scheme of a specular GMR stack; (b) TEM image of a specular GMR stack with Ta (1.5nm)/NiFeCr (3 nm)/PtMn (12 nm)/CoFe (1.8nm)/Ru(0.85 nm)/CoFe (1 nm)/Nano oxides layer (NOL, 1.3 nm)/CoFe (2 nm)/Cu (2.1 nm)/CoFe (0.8 nm)/NiFe(1.5 nm)/Cu0.8nm/Ta(1.2 nm) layers; (c) The transfer curve of the specular GMR full film with a MR value of 16% and a maximum sensitivity of 1.6% Oe^{-1} in a 10 Oe field.

by BSA. The longitude MR transfer curve is shown in Figures 4c and 4d as well. The longitudinal curve exhibited the same trend as did the transverse field, and a 0.5% MR drop was observed.

To deduce the dynamic range of signal versus concentration scaling relationship, a series of quantitative calibration experiments employing varying carcinoembryonic antigen (CEA) concentration were conducted. CEA analyte was diluted in a PBS buffer to produce analyte concentrations ranging from 1 ng/mL (molar concentration 5 pM) to 1 pg/mL (molar concentration 5 fM). Eight solutions containing between 5 fM to 500 pM CEA analyte were using for testing of the sensor system. Each of the 8 solutions was pipetted onto five active sensors on the array. From the CEA concentration and sensor signal, the linear response curve (on a log–log plot) shown in Figure 5 was created. Linearity of response was obtained even at the fM concentration. These results indicate that detection of CEA is possible down to the fM-level without any biological amplification. This dynamic range of linearity is comparable to the best GMR-based detecting [30,42] and is three orders of magnitude higher than conventional ELISA (4 pM) [43-45].

Discussion

The enhancement of NOL (nano-oxide-layer) insertion and specular effects on the giant magnetoresistance (GMR) can be explained by the semiclassical Boltzmann theory. Spin valves (SVs) consist of two ferromagnetic (FM) nanolayers separated by a non-magnetic spacer. One of the FM layers is pinned by an adjacent AFM layer, while the other (free layer) rotates its magnetization (M) under a small magnetic field. This allows both magnetizations either parallel (low resistance) or antiparallel (high resistance) to be obtained with an externally applied magnetic field. The nano-oxide layer NOL inserted either adjacent to the pinned layer or free layers [46-48] can highly enhance the majority spin orientated electrons specularly scatter at NOL [49,50] and thus a high dR/R.

In order to support the observations in this study, the theoretical magnetic stray field of a fully magnetized 15 nm diameter Fe_3O_4 nanoparticle was calculated at different distances from the free layer of GMR sensor. The stray field, H, of a magnetic dipole of length l placed perpendicularly on top of the sensing area of the GMR sensor at a distance d is approximated by the following formula (the case that d >>l in CGS units by Bozorth [51]

$$H = \frac{M}{d^3}\left(1 - \frac{3l^2}{4d^2}\right) \quad (1)$$

With M being the magnetic moment (5×10^{-18} emu, of a single Fe_3O_4 nanoparticle from SQUID measurement at 100 Oe), and l is the characteristic particle dimension (in this case the 15 nano meter diameter). The calculation shows the theoretical active distance of the sensor (at 3×10^{-4} Oe) lies between 200 and 250 nm above the sensor. The stray field of the 2 Oe observed in Figure 4b, in principle, can be produced by 6×10^4 magnetic nanoparticles of size 15 nm passing the sensor at a height of approximately 200 nm. To further enhance the detecting sensitivity of GMR bioassay, decreasing the distance between MNP and the free layer of the sensor is critical too.

The 15 nm MNP-based specular GMR assay presents a very sensitive magnetic detection method for protein arrays. With carefully screened antibodies, the sensitivity and selectivity of the MNP-based specular GMR assay is already sufficient for clinically relevant protein detection in real world serum samples [52,53]. The technique can be readily performed with the multiplex protein detection. Individual sensor microspotting will allow the accommodation and measurement of up to 22000 different probes

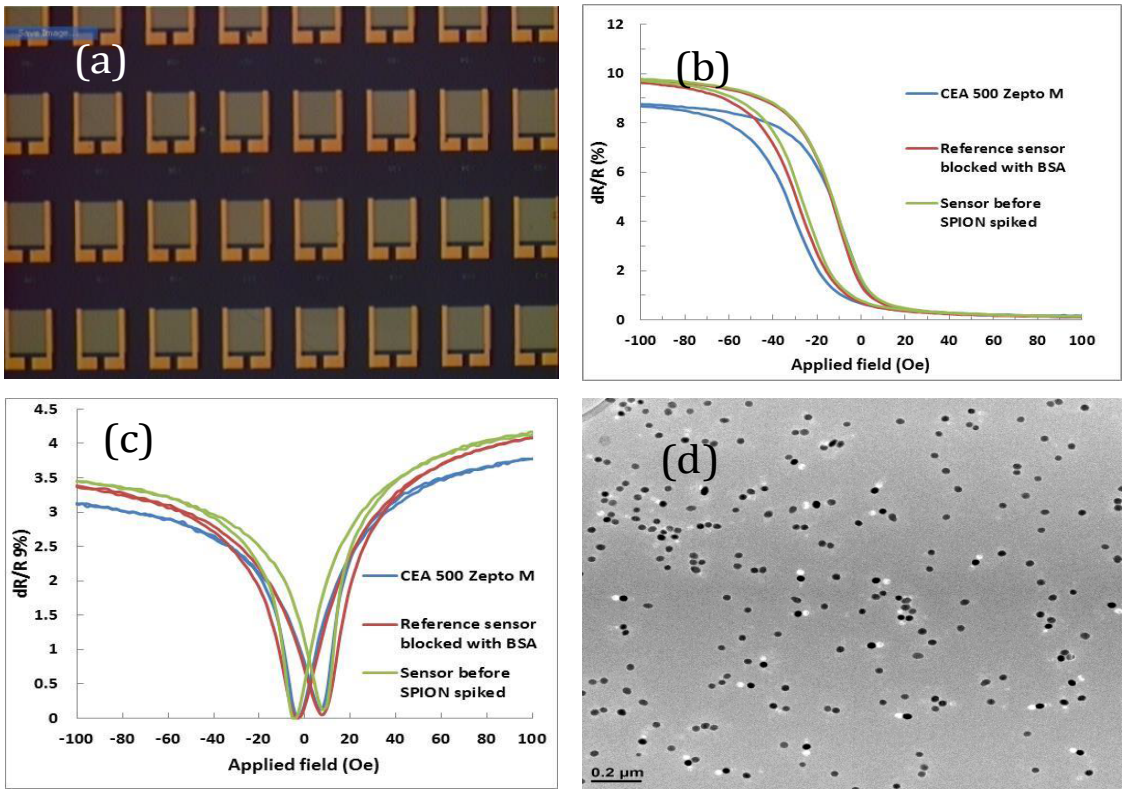

Figure 4: (a) The optical images of a patterned GMR bioarray; **(b)** MR transfer loop of a GMR bioarray before and after MNPs spiked along with sensors with BSA blocking under a magnetic field along the hard-axis bias (transverse); **(c)** MR transfer loop of a GMR bioarray before and after MNPs spiked along with sensors with BSA blocking under a magnetic field along the easy-axis bias (Longitude). **(d)** TEM images of the MNP spiked on the sensor surface.

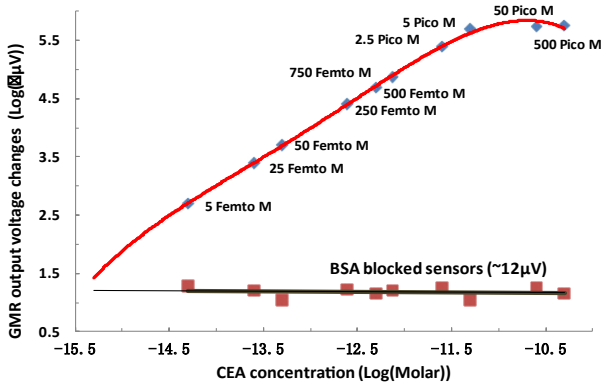

Figure 5: Graph of GMR sensor resistance deviations with axis of ΔR versus iron–oxide MNP concentrations. The fitting curve (solid line) designates that the resistance deviation of the GMR sensor changes logarithmically with MNP concentration.

on a current generation chip (probing throughput not withstanding). It is expected that significant sensitivity improvements can also be made on the sensor; for example, using either a biased magnetic tunnel junction sensors based on MgO barrier or by using sensors with smaller geometry [54]. In the near future, capture agents with higher affinity, and similarly small but higher magnetic moment MNPs are expected to further enhance the analytic sensitivity of MNP-based assays.

In conclusion, the highly sensitive detection of protein tumor markers incorporating a MNP based specular GMR bio-assay was demonstrated. Also, it was demonstrated the detecting system can adopt the principle of ELISA assay with improved sensitivity. The GMR bioarray, permits real-time measurements of CEA protein concentrations down to the femtomolar level with a linear dynamic range of over five orders of magnitude. This GMR- and magnetic-nanoparticle based detecting system, therefore, is expected to be applicable to many other biological systems for detection and quantification of various biomolecules. The high sensitivity of this detecting system opens new paths for the detection of biomolecules involved in the etiology of various diseases. Most importantly, the magnetic/electric nature of this detecting system and the associated cost benefit, scalability and versatility will help the realization of personalized medicine.

Author contributions statements: NY carried out the sample preparation and experimental measurements. TL and PPZ help to analyze the experimental result. HYF drafted the manuscript. XQC and WZ conceived and designed the experiments, revised the manuscript, and provided financial support. All authors read, review and approved the final manuscript.

Competing financial interests

The authors declare no competing financial interests.

Acknowledgements

This work was supported in part by Jiangsu Province Key Project for Society Development under contract BE2012759, National High Technology Development Program under contract 2014AA020604 and a Project Funded by the Priority Academic Program Development of Jiangsu Higher Education Institutions (PAPD).

References

1. Atkinson AJ, Colburn WA, DeGruttola VG, DeMets DL, Downing GJ, et al. (2001) Biomarkers and surrogate endpoints: preferred definitions and conceptual framework. Clin Pharmacol Ther 69: 89-95.
2. Cancer Diagnosis (2008) Information about Cancer, Stanford Cancer Center.
3. CEA: the test (2013) Lab Tests Online (USA). American Association for Clinical Chemistry.
4. Engvall E, Perlmann P (1972) Enzyme-linked immunosorbent assay, Elisa. 3. Quantitation of specific antibodies by enzyme-labeled anti-immunoglobulin in antigen-coated tubes. J Immunol 109: 129-135.
5. Engvall E (1980) Enzyme immunoassay ELISA and EMIT. Methods Enzymol 70: 419-439.
6. Zheng G, Patolsky F, Cui Y, Wang WU, Lieber CM (2005) Multiplexed electrical detection of cancer markers with nanowire sensor arrays. Nat Biotechnol 23: 1294-1301.
7. Ghosh S, Sood AK, Kumar N (2003) Carbon nanotube flow sensors. Science 299: 1042-1044.
8. Drummond TG, Hill MG, Barton JK (2003) Electrochemical DNA sensors. Nat Biotechnol 21: 1192-1199.
9. Chan SM, Ermann J, Su L, Fathman CG, Utz PJ (2004) Protein microarrays for multiplex analysis of signal transduction pathways. Nat Med 10: 1390-1396.
10. Shingyoji M, Gerion D, Pinkel D, Gray JW, Chen F (2005) Quantum dots-based reverse phase protein microarray. Talanta 67: 472-478.
11. Lee JR, Magee DM, Gaster RS, LaBaer J, Wang SX (2013) Emerging protein array technologies for proteomics. Expert Rev Proteomics 10: 65-75.
12. Tang L, Casas J, Venkataramasubramani M (2013) Magnetic nanoparticle mediated enhancement of localized surface plasmon resonance for ultrasensitive bioanalytical assay in human blood plasma. Anal Chem 85: 1431-1439.
13. Bruce IJ, Sen T (2005) Surface modification of magnetic nanoparticles with alkoxysilanes and their application in magnetic bioseparations. Langmuir 21: 7029-7035.
14. Huang YF, Wang YF, Yan XP (2010) Amine-functionalized magnetic nanoparticles for rapid capture and removal of bacterial pathogens. Environ Sci Technol 44: 7908-7913.
15. Deng Y, Qi D, Deng C, Zhang X, Zhao D (2008) Superparamagnetic high-magnetization microspheres with an Fe_3O_4@SiO_2 core and perpendicularly aligned mesoporous SiO2 shell for removal of microcystins. J Am Chem Soc 130: 28-29.
16. Scarberry KE, Dickerson EB, McDonald JF, Zhang ZJ (2008) Magnetic nanoparticle-peptide conjugates for in vitro and in vivo targeting and extraction of cancer cells. J Am Chem Soc 130: 10258-10262.
17. Earhart CM, Hughes CE, Gaster RS, Ooi CC, Wilson RJ (2014) Isolation and mutational analysis of circulating tumor cells from lung cancer patients with magnetic sifters and biochips. LAB ON A CHIP 14: 78-88.
18. Cho NH, Cheong TC, Min JH, Wu JH, Lee SJ, et al. (2011) A multifunctional core-shell nanoparticle for dendritic cell-based cancer immunotherapy. Nat Nanotechnol 6: 675-682.
19. Nagaoka H, Sato Y, Xie X, Hata H, Eguchi M (2011) Coupling stimuli-responsive magnetic nanoparticles with antibody-antigen detection in immunoassays. Anal Chem 83: 9197-9200.
20. Kitz R, Matz H, Trahms L (1997) SQUID based remanence measurements for immunoassays. IEEE Trans. Appl. Supercon 7: 3678-3681.
21. Baselt DR, Lee GU, Natesan M, Metzger SW, Sheehan PE, et al. (1998) A biosensor based on magnetoresistance technology. Biosens Bioelectron 13: 731-739.
22. Edelstein RL, Tamanaha CR, Sheehan PE, Miller MM, Baselt DR (2000) The BARC biosensor applied to the detection of biological warfare agents. Biosens Bioelectron 14: 805-813.
23. Taton K, Johnson D, Guire P, Lange E, Tondra M (2009) Lateral flow immunoassay using magnetoresistive sensors. J Magn Magn Mater 321: 1679-1682.
24. Marquina C, MdeTeresa J, Serrate D, Marzo, Cardoso FA, et al. (2012) GMR sensors and magnetic nanoparticles for immune-chromatographic assays. J Magn Magn Mater 324: 3495-3498.
25. Mak AC, Osterfeld SJ, Yu H, Wang SX, Davis RW, et al. (2010) Sensitive giant magnetoresistive-based immunoassay for multiplex mycotoxin detection. Biosens Bioelectron 25: 1635-1639.
26. Yang HW, Lin CW, Hua MY, Liao SS, Chen YT, et al. (2014) Combined detection of cancer cells and a tumor biomarker using an immunomagnetic sensor for the improvement of prostate-cancer diagnosis. Adv Mater 26: 3662-3666.
27. Wang Y, Wang W, Yu L, Tu L, Feng Y, et al. (2015) Giant magnetoresistive-based biosensing probe station system for multiplex protein assays. Biosensors and Bioelectronics70: 61-68.
28. Wang T, Yang Z, Lei C, Lei J, Zhou Y, et al. (2014) An integrated giant magnetoimpedance biosensor for detection of biomarker. Biosens Bioelectron 58: 338-344.
29. Hall DA, Gaster RS, Lin T, Osterfeld SJ, Han S, et al. (2010) GMR biosensor arrays: a system perspective. Biosens Bioelectron 25: 2051-2057.
30. Gaster RS, Hall DA, Nielsen CH, Osterfeld SJ, Yu H, et al. (2009) Matrix-insensitive protein assays push the limits of biosensors in medicine. Nat Med 15: 1327-1332.
31. Cabral JMS, Ferreira HA, Freitas PP, Graham DL (2003) Biodetection using magnetically labeled biomolecules and arrays of spin valve sensors (invited). Journal of Applied Physics 93: 7281-7286.
32. Miller MM, Rife JC, Sheehan PE, Tamanaha CR, Tondra M, et al. (2003) Design and performance of GMR sensors for the detection of magnetic microbeads in biosensors. Sensors and Actuators A: Physical 107: 209-218.
33. Becker A, Brueckl H, Brzeska M, Huetten A, Kamp PB, et al. (2005) Magnetoresistive sensors and magnetic nanoparticles for biotechnology. Journal of Materials Research 20: 3294-3302.
34. Koets M, van der Wijk T, van Eemeren JT, van Amerongen A, Prins MW (2009) Rapid DNA multi-analyte immunoassay on a magneto-resistance biosensor. Biosens Bioelectron 24: 1893-1898.
35. Gaster RS, Xu L, Han SJ, Wilson RJ, Hall DA, et al. (2011) Quantification of protein interactions and solution transport using high-density GMR sensor arrays. Nat Nanotechnol 6: 314-320.
36. Prinz GA (1998) Magnetoelectronics Science 282: 1660-1663.
37. Li Y, Srinivasan B, Jing Y, Yao X, Hugger MA, et al. (2010) Nanomagnetic competition assay for low-abundance protein biomarker quantification in unprocessed human sera. J Am Chem Soc 132: 4388-4392.
38. Griffiths DJ (1981) Introduction to electrodynamics. Prentice Hall, Englewood Cliffs N. J: 07632 second edition.
39. Zhang GJ, Tanii T, Zako T, Funatsu T, Ohdomari, et al. (2004) The immobilization of DNA on microstructured patterns fabricated by maskless lithography. Sens Actuat B 97: 243-248.
40. Xu YH, Bai J, Wang JP (2007) High-magnetic-moment multifunctional nanoparticles for nanomedicine applications. J Magn Magn Mater 311: 131-134.
41. Srinivasan B, Li Y, Jing Y, Xu YH, Yao XF, et al. (2009) A Detection System Based on Giant Magnetoresistive Sensors and High-Moment Magnetic Nanoparticles Demonstrates Zeptomole Sensitivity: Potential for Personalized Medicine. Chem Int Ed 48: 2764-2767.
42. Mathivanan (2007) PC-based Instrumentation: Concepts and Practice: Prentice. Hall Of India Pvt Limited.
43. Li G, Sun S, Wilson RJ, White RL, Pourmand N, et al. (2006) Spin valve sensors for ultrasensitive detection of superparamagnetic nanoparticles for biological applications. Sens Actuators A Phys 126: 98-106.
44. Schotter J, Kamp PB, Becker A, Pühler A, Reiss G, et al. (2004) Comparison of a prototype magnetoresistive biosensor to standard fluorescent DNA detection. Biosens Bioelectron 19: 1149-1156.
45. Shen W, Schrag BD, Carter MJ, Xiao G (2008) Quantitative detection of DNA labeled with magnetic nanoparticles using arrays of MgO-based magnetic tunnel junction sensors. Appl Phys Lett 93: 033903.

46. Veloso A, Freitas PP, Wei P, Barradas NP, Soares JC, et al. (2000) Magnetoresistance enhancement in specular, bottom-pinned, Mn83Ir17spin valves with nano-oxide layers. Appl Phys Lett 77: 1020-1022.

47. Wang L, Qiu J J , McMahon WJ, Li KB , Wu YH, et al. (2004) Nano-oxide-layer insertion and specular effects in spin valves: Experiment and theory. Phys Rev B 69: 214402-16.

48. Varadan VK, Chen L, Xie J (2008) Nanomedicine, Design and Applications of Magnetic Nanomaterials, Nanosensors and Nanosystems. Chichester Wiley.

49. Guimaraes AP (2009) Principles of Nanomagnetism. Springer Berlin Heidelberg.

50. Bean CP, Livingston JD (1959) Superparamagnetism. J Appl Phys 30: 120-129.

51. Bozorth RM (1951) Ferromagnetism. Van Nostrand.

52. Martins VC, Cardoso FA, Germano J, Cardoso S, Sousa L, et al. (2009) Femtomolar limit of detection with a magnetoresistive biochip. Biosens Bioelectron 24: 2690-2695.

53. Carter MJ, Schrag BD, Shen W, Sun H, Xie J, et al. (2008) Detection of DNA labeled with magnetic nanoparticles using MgO-based magnetic tunnel junction sensors. J Appl Phys 103: 07A306.

54. Kingsmore SF (2006) Multiplexed protein measurement: technologies and applications of protein and antibody arrays. Nat Rev Drug Discov 5: 310-320.